CHEMICAL ENGINEERING TRANSACTIONS
VOL. 116, 2025
A publication of AIDIC
The Italian Association of Chemical Engineering
Online at www.cetjournal.it
Guest Editors: Bruno Fabiano, Valerio Cozzani

ISBN 979-12-81206-18-2; **ISSN** 2283-9216
DOI: 10.3303/CET25116034

Advanced Boundary Conditions for the Simulation of Fire Engulfment Tests of Cryogenic Storage Tanks

Alice Schiaroli[a,b*], Giordano E. Scarponi[a], Christian Mata[c], Federico Ustolin[b], Valerio Cozzani[a]

[a] LISES – Laboratory of Industrial Safety and Environmental Sustainability – Department of Civil, Chemical, Environmental and Materials Engineering – University of Bologna, via Terracini 28, 40131, Bologna, Italy
[b] Norwegian University of Science and Technology – NTNU – Department of Mehcanical and Industrial Engineering. Richard Birkelands vei 2, 7034, Trondheim, Norway
[c] Research Centre for Biochemical Engineering (CREB), Universitat Politècninca de Catalunya, 08028, Barcelona, Spain
alice.schiaroli@unibo.it

The fire engulfment of a cryogenic storage tank can be simulated using mathematical models. Currently, the available approaches reproduce the real case scenario considering a static full engulfment of the component. Unfortunately, given the dynamic nature of the fire, this simplification is often far from reality, primarily for fires in open environments where wind strongly affects the flame distribution on the tank surface. This study applies a digital image processing technique to replicate the time-varying partial engulfment of a cryogenic storage tank tested in external fire conditions. The obtained results are used to define dynamic boundary conditions implemented in a lumped model to estimate the pressurization and heating of the component during the fire attack. The study highlights the improved accuracy in the characterization of the fire obtainable with the present approach and emphasizes the need for a precise characterization of the system to correctly replicate the experimental data.

1. Introduction

In formulating mathematical models to predict the response of storage tanks engulfed in fires, defining boundary conditions representative of the fire engulfment poses significant challenges. Currently, most available approaches assume a complete fire engulfment of the target, defining a uniform flame temperature all over its outer surface. However, this assumption neglects fundamental aspects and does not represent real fire accident scenarios that typically involve a partial inhomogeneous fire engulfment, varying with time (Scarponi et al., 2024).. Furthermore, when considering fires in the open air, the approach becomes even less realistic as it disregards the effect of the wind speed (Oka et al., 2003) and direction on the flame distribution around the component (Espinosa et al., 2019). As demonstrated in previous studies, the engulfment mode, including the engulfment level and the position of the flame, strongly affects the tank thermal response, especially in terms of self-pressurization (Scarponi et al., 2024). Thus, the definition of realistic boundary conditions is crucial for a correct modelling. To address the existing abovementioned limitations, Digital Image Processing (DIP) can be used. The method involves a series of consecutive image manipulations to extract data from a digital image (Seeram, 2019) and has already been used in the context of fire safety to investigate various fire scenarios, including fire detection in forests (Chi et al., 2015) and cities (Sharma et al., 2020), and the characterization of the flame in terms of brightness and velocity (Rashidi et al., 2015). A preliminary application of this method on the recordings of an experimental fire test involving cryogenic storage tanks demonstrated the capability of the technique to extract time and space-dependent flame coverage (Schiaroli et al., 2023). In the present study, the preliminary analysis is refined to obtain a dynamic partial fire engulfment condition, reproducing with high fidelity the actual test. Then, the retrieved information is used to investigate how the definition of dynamic boundary conditions reflects on the modelling of the tank behaviour during the fire attack. For this purpose, a lumped

Paper Received: 18 November 2024; Revised: 1 February 2025; Accepted: 14 April 2025
Please cite this article as: Schiaroli A., Scarponi G.E., Mata C., Ustolin F., Cozzani V., 2025, Advanced Boundary Conditions for the Simulation of Fire Engulfment Tests of Cryogenic Storage Tanks, Chemical Engineering Transactions, 116, 199-204 DOI:10.3303/CET25116034

model is used. The boundary conditions in the model are defined based on the results of the DIP, and the outcomes are compared with the ones obtained under the assumption of static full engulfment.

2. Methodology

The definition of dynamic boundary conditions aims at reproducing closely the fire engulfment of the storage tank and providing an accurate estimation of its behavior. In the present analysis, a simplified digital image processing is performed to calculate the tank flame coverage (i.e., the fraction of the total tank surface covered by the flames) during the fire exposure. Then, the results are implemented in a mathematical model able to quantify the pressure build-up and outer temperature of the target tank. The scheme of the methodology is shown in Figure 1, where the steps highlighted in blue (from 1 to 4) refer to the simplified DIP. The method is intended to be applied to images extracted at different times from the video recordings of a fire test involving a storage tank and showing the component from different views (e.g., North, South, West, East, Up and Down). The procedure described in the following must be repeated for each tank view and for the different times selected for the frame extraction.

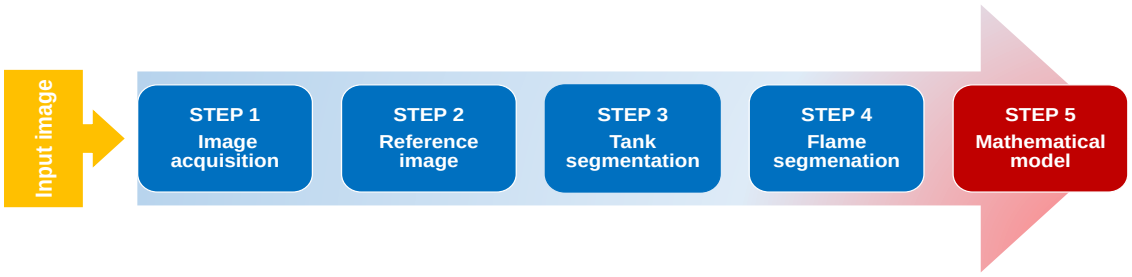

Figure 1: Scheme of the methodology used in the present study; steps from 1 to 4 (in blue) are part of the simplified Digital Image Processing.

First, the input images extracted from the video recordings are acquired in a computer and converted into a 2D numerical matrix I(m,n) (STEP 1). Then, the reference image is created from a pre-fire image (i.e., an image showing the tank not covered by the flames) isolating the tank surface (STEP 2). Then, combining grayscale conversion, edge detection and morphological operations, the reference image is segmented and converted into the tank mask, where the object of interest (i.e., the tank section) is depicted as white and the rest is included in the background and shown as black (STEP 3). At this point, the tank mask is used to locate and isolate the tank section in the images extracted during the fire exposure. Then, the segmentation is repeated to isolate the flame from the tank by thresholding high-intensity values in the red channel and obtain the flame mask (STEP 4). The output of this step is a black image where the flame is depicted in white. After that, the average flame coverage (FC) of the tank at a fixed time interval is obtained as:

$$FC(t) = \sum_{i}^{n} \frac{A_i}{A_{TOT}} \times \frac{N° \; of \; pixels \; in \; the \; flame \; mask_i(t)}{N° \; of \; pixels \; in \; the \; tank \; mask_i} \quad (1)$$

Where A_i is the area of the ith view of the tank (i.e., North, South, West, and East), A_{TOT} is the total outer surface of the tank, t is the time at which the frames are extracted, and n is the number of tank views. The resulting time-varying flame coverage of the component is used to reproduce the dynamic partial engulfment in a mathematical model. Since the goal of the study is to demonstrate the importance of accurately defining boundary conditions rather than precisely reproduce the thermodynamic phenomena inside the tank, a lumped model is preferred over computational fluid dynamic ones due to the lower computational effort required. In the model, the domain is divided into three thermal nodes, as shown in Figure 2.

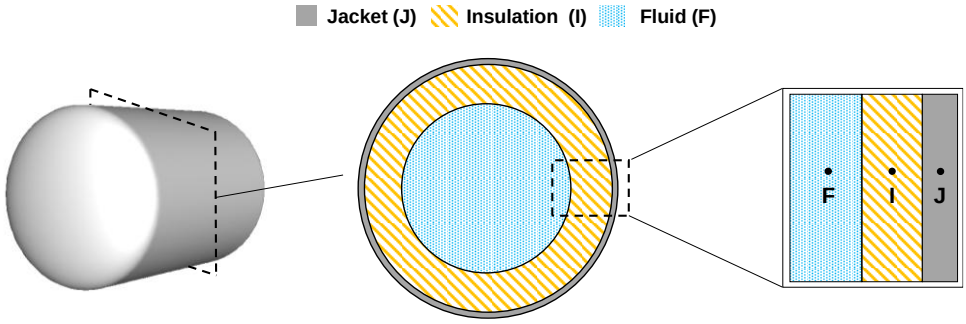

Figure 2. Discretization of the domain in the lumped model; F = fluid; I = insulation; J = jacket.

The equations solved in the model are summarized in Table 1, where the subscripts f, i, and j refer to the fluid, the insulation, and the jacket, respectively. In the first equation, A_f is the surface of the tank in contact with the fluid in m^2.

Table 1: Equations solved for the three nodes in the lumped model; F = fluid; I = insulation; J = jacket; m=mass (kg), U=internal energy (J), t=time (s), k=thermal conductivity (W m^{-1} K^{-1}), δ=thickness (m), T=temperature (K), cp=specific heat (J kg^{-1} K^{-1}), ρ=density (kg m^{-3}).

Node	Variable	Variable symbol	Equation
F	Fluid Internal energy	U	$m_f \frac{dU_f}{dt} = A_f \frac{k_i}{\frac{\delta_i}{2}}(T_i - T_f)$
I	Insulation temperature	Ti	$\rho_i cp_i \delta_i \frac{dT_i}{dt} = \frac{k_i}{\frac{\delta_i}{2}}(T_j - T_i) - \frac{k_i}{\frac{\delta_i}{2}}(T_i - T_f)$
J	Jacket temperature	Tj	$\rho_j cp_j \delta_j \frac{dT_j}{dt} = Irr - \frac{k_i}{\frac{\delta_i}{2}}(T_j - T_i)$

The data relative to the flame coverage are implemented in the model to define the radiative heat flux received from the tank due to the fire engulfment:

$$Irr = \sigma\varepsilon_j\left(\varepsilon_{flame}T_{flame}^4 \times FC + (1 - FC)T_{ambient}^4\right) - \left(\sigma\varepsilon_j T_j^4\right) \quad (2)$$

Where σ is the Stefan-Boltzmann constant, ε_{flame} is the flame emissivity, ε_j is the jacket emissivity, and T_{flame} and $T_{ambient}$ (293.15 K) are the flame and ambient temperature in K, respectively.

3. Case study

In this study, one of the three fire tests carried out during the Safe Hydrogen Fuel Handling and Use for Efficient Implementation (SH2IFT) project at the Federal Institute for Materials Research and Testing (BAM) in Berlin is simulated (Ødegård et al., 2022). The fire test involved a horizontal double-walled cryogenic storage tank insulated with perlite under a high vacuum (0.3 mbar). The inner and outer shells of the tank were made of low-temperature resistant stainless steel and had a thickness of 3 mm and 4 mm, respectively; the insulation space between the shells was 217.4 mm thick. The amount of liquid hydrogen stored was around 30 kg, corresponding to a filling degree of 40%. The fire engulfment was reproduced by 36 propane burners (flame temperature of 1,193 K (Pehr, 1996)) placed below the vessel. The maximum pressure inside the tank was observed at around 4,500 seconds from the beginning of the test, before a quick drop was measured due to an unexpected leak in the system; at that time, the measured vacuum pressure in the insulation space was 0.06 mbar. For the fire test, the video recordings were available for the North, South, East and West views of the tank (n=4 in Eq. (1)).
Assumptions are introduced to obtain the missing input data necessary for the model. The insulation is characterized by a density of 100 kg m^{-3} and a specific heat of 840 J kg^{-1} K^{-1}. Different values for the perlite thermal conductivity, calculated following the procedure provided by Clark (1969), are tested to assess how the variation in the boundary conditions reflects on the tank pressurization and how this impact is related to the insulation performance. The values are summarized in Table 2, where P1 and P3 represent perfectly working systems (i.e., vacuum pressure unchanged), while P2 and P4 represent degraded systems (i.e., increased

vacuum pressure in the insulation annular space). The pressure relief valve is not simulated to replicate the worst-case scenario.

Table 2: Properties of the perlite insulation considered in the present study in the lumped model.

Case ID	P1	P2	P3	P4	Reference
Vacuum pressure (mbar)	0.03	0.06	0.03	0.06	(Ødegård et al., 2022)
Particles diameter (mm)	0.08	0.08	0.1	0.1	(Rottmann and Beikircher, 2022)
Porosity	0.93	0.93	0.99	0.99	(Rottmann and Beikircher, 2022)
Thermal conductivity (W m^{-1} K^{-1})	**0.016**	**0.091**	**0.024**	**0.495**	(Clark, 1969)

4. Results and discussion

In this study, the images for the DIP application are extracted from the recordings of the experimental fire test with an interval of 20 seconds. An example of the results of the DIP is presented in Figure 3. As shown for the East view, applying the method on pre-fire images allows the isolation of the tank surface and the following creation of the tank mask while the flame is detected and distinguished from the rest of the image starting from a frame obtained during the fire engulfment. The number of pixels in the tank and flame regions is calculated summing the white pixels in their respective masks, providing quantitative area measurements.

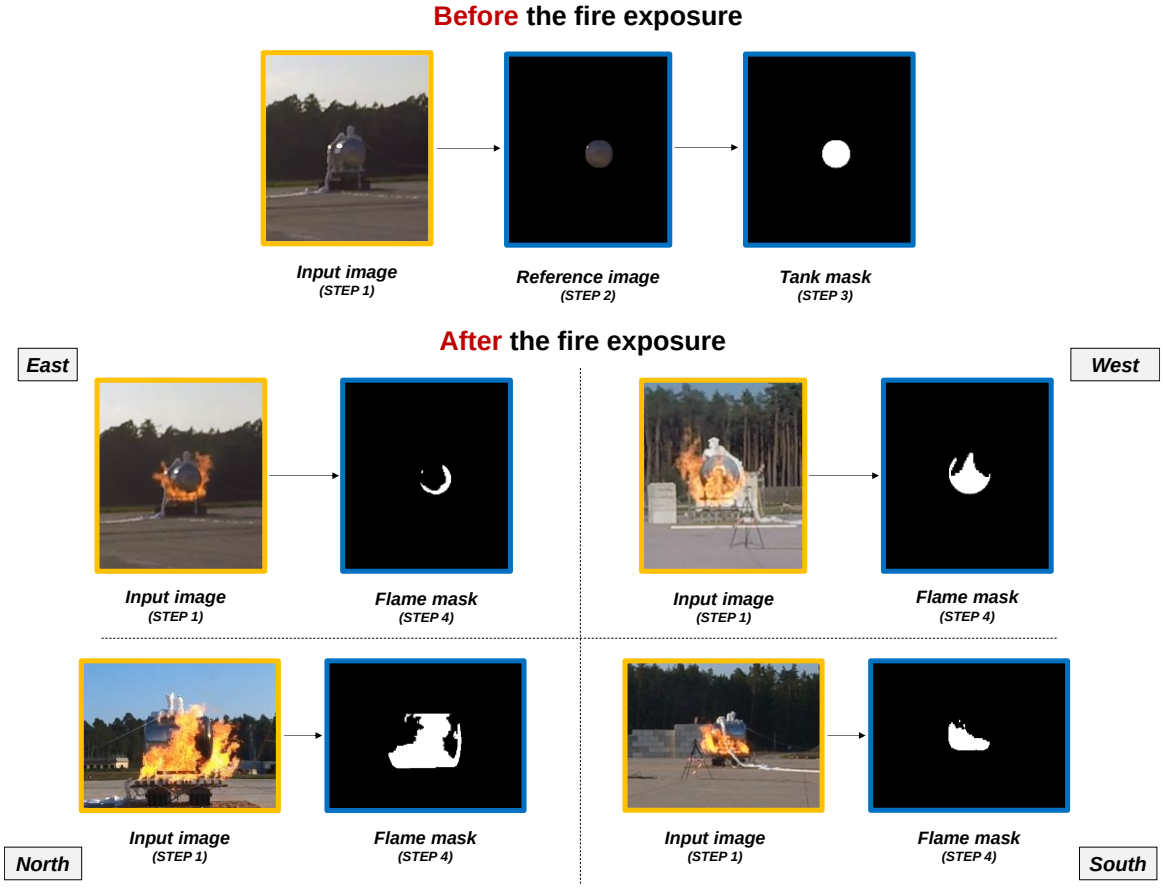

Figure 3: Results of the digital image processing applied on the images extracted from the video recordings of the experimental fire test BLEVE01; the frames with the fire are extracted after 80 s from the test start.

The flame mask in Figure 3 shows that the fire does not completely cover the tank in any of the views and demonstrates that the flame distribution around the component is strongly inhomogeneous. Moreover, even if the results are shown for a specific time (80 seconds from the beginning of the test), the effect of the wind on the flame coverage can be observed. In fact, in the input image for the North and South view, the fire is clearly shifted to West. Therefore, the West surface of the tank is more covered by the flames than the East one. With data obtained from the DIP, an average flame coverage of 0.67 is calculated for the test. Considering that a

value of 1 indicates a complete fire engulfment, the result confirms that the assumption of a full and static engulfment is inaccurate to reproduce the experiment and significantly overestimates the actual tank surface covered by the flame.
Figure 4a shows the pressurization of the storage tank calculated with the lumped model for the four case studies.

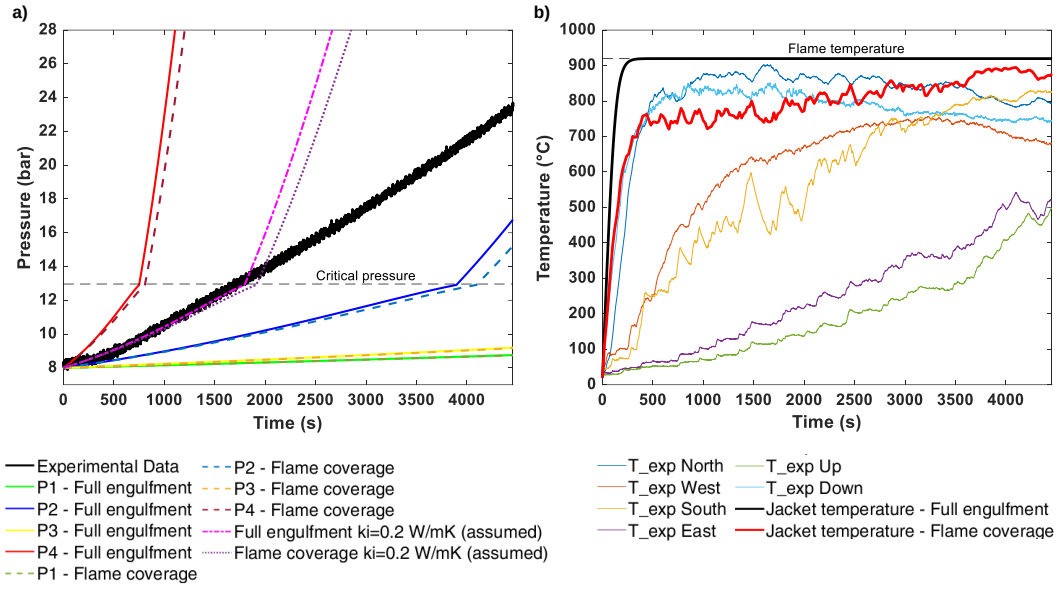

Figure 4: a) Pressurization of the storage tank during the fire engulfment in the BLEVE01 test; b) Temperature of the tank jacket; exp=experimental.

For case studies P1, P2, and P3, the results obtained with the full engulfment and the variable flame coverage assumptions are very similar, while a more considerable difference is observed for case P4. This is explained by considering that in the case of well-performing insulation (i.e., low thermal conductivity as in cases P1, P2, and P3), the heat provided by the fire is effectively shielded, leading to negligible differences (in absolute terms) in the heat flux received by the fluid. In contrast, when the thermal performance of the insulation is compromised due to degradation (i.e., high thermal conductivity, as in case P4), the differences in the heat flux at the outer wall are not mitigated. Thus, the reduction in the engulfment level on the outer tank wall is clearly reflected in a lower heat flux to the inner fluid and in the consequent lower pressure build-up. Regardless of the insulation performance and the boundary conditions, the model predictions do not agree with the experimental data. Specifically, with the assumption of a perfectly working insulation (P1 and P3) the inner pressure is strongly underestimated. The same is true for case P2, although a certain degree of degradation was considered. On the other hand, the worst insulation performance selected in this study (P4) leads to a significant overestimation of the pressure build-up. These results show that none of the case study configurations selected in this study correctly characterize the perlite used in the experimental test. Therefore, in addition to the accurate characterization of the fire scenario, given the strong influence of the insulation performance on the tank response, a precise description of the relevant insulation features is fundamental to reproducing the fire test and providing a meaningful analysis of the tank behavior. A first attempt is made in this study, investigating additional cases for the perlite thermal conductivity. A good agreement with the experimental data is found with a value of 0.2 W m^{-1} K^{-1} when the fluid is in subcritical condition. The deviation of the curves above the critical pressure could be a consequence of the fact that above the critical point the liquid phase is no longer considered in the model, and the entire fluid content is assumed to be in the gaseous phase. Despite that, this result indicates that during the test the insulation performance was intermediate among the ones considered in this study.
The results for the tank outer temperature are presented in Figure 4b, where they compared with the experimental data. Unlike the full engulfment approach, the method proposed in this study captures temperature peaks and lows over time, better resembling the experimental trends. It must be remarked that the temperature calculated by the lumped model is the average value across the tank outer surface. Thus, the comparison with the experimental curves reveals that the different tank surfaces do not equally contribute to the average tank temperature. In this case, the red line approaches the values of the North and Down views following the increasing trend of the South view, suggesting that the average jacket temperature is predominantly influenced

by these measurements and indicating that the average value is not sufficient to represent the tank heating due to the strong inhomogeneous temperature distribution.

5. Conclusions

This study provides an advanced method to define dynamic boundary conditions suitable to reproduce a realistic fire exposure of a storage tank in a mathematical model. The use of these conditions in a lumped model highlights the importance of a precise fire characterization, especially in case of compromised insulation performance. The analysis proposed in this study can be improved by reproducing the real flame mask obtained from the image processing on a three-dimensional geometry of the tank. The thermodynamic of the fluid can be further investigated adding nodes to the lumped model to better capture the temperatures and heat flux and temperature variations in the system. Finally, the same analysis could be performed considering a more complex and accurate mathematical approach, such as a computational fluid dynamic one.

Acknowledgments

This work was undertaken as part of the research project Safe Hydrogen Fuel Handling and Use for Efficient Implementation 2 (SHIFT-2), and the authors would like to acknowledge the financial support of the Research Council of Norway under the ENERGIX programm (Grant No. 327009). This work was undertaken as part of the ELVHYS project No. 101101381 supported by the Clean Hydrogen Partnership and its members. UK participants in Horizon Europe Project ELVHYS are supported by UKRI gran numbers 10S063519 (University of Ulster) and 10070592 (Health and Safety Executive). Funded by the European Union Views and opinions expressed are however those of the author(s) only and do not necessarily reflect those of the European Union or Clean Hydrogen JU. Neither the European Union nor the granting authority can be held responsible for them.

References

Chi, Y., Liu, Z., Zhang, Y., 2015. UAV-based Forest Fire Detection and Tracking Using Digital Processing Techniques. Int. Conf. Unmanned Aircr. Syst. 639–643.

Clark, J.A., 1969. Cryogenic Heat Transfer, in: Irvine, T.F., Hartnett, J.P.B.T.-A. in H.T. (Eds.), . Elsevier, pp. 325–517. https://doi.org/https://doi.org/10.1016/S0065-2717(08)70132-1

Espinosa, S.N., Jaca, R.C., Godoy, L.A., 2019. Thermal effects of fire on a nearby fuel storage tank. J. Loss Prev. Process Ind. 62, 103990. https://doi.org/https://doi.org/10.1016/j.jlp.2019.103990

Ødegård, A., Sommerseth, C., Odsæter, L.H., Skarsvåg, H.L., Nekså, P., Meraner, C., Stølen, R., Li, T., Muthusamy Deiveegan, Van Wingerden, K., Siccama, D., Gawas, Y., Ustolin, F., George, C., 2022. D5.4: SH2IFT final project report.

Oka, Y., Sugawa, O., Imamura, T., Matsubara, Y., 2003. Effect of cross-winds to apparent flame height and tilt angle from several kinds of fire source. Fire Saf. Sci. 915–926. https://doi.org/10.3801/IAFSS.FSS.7-915

Pehr, K., 1996. EXPERIMENTAL EXAMINATIONS ON THE WORST CASE BEHAVIOUR OF LH2/LNG TANKS FOR PASSENGER CARS.

Rashidi, A., Ahmad, A., Lou, C., Hassan, H., Hariffin, M., Tzeng, M., Akma, N., Der, S., 2015. Preliminary determination of flame speeds from infrared images using image processing techniques in a 150 kWth coal fired combustion test rig. Institute of Research Engineers and Doctors, LLC, pp. 1–5. https://doi.org/10.15224/978-1-63248-072-9-50

Rottmann, M., Beikircher, T., 2022. Pressure dependent effective thermal conductivity of pure and SiC-opacified expanded perlite between 293 K and 1073 K. Int. J. Therm. Sci. 179. https://doi.org/10.1016/j.ijthermalsci.2022.107652

Scarponi, G.E., Cozzani, V., Antonioni, G., Doghieri, F., 2024. Modeling the behavior of LPG tanks exposed to partially engulfing pool fires. Process Saf. Environ. Prot. 182, 1072–1085. https://doi.org/https://doi.org/10.1016/j.psep.2023.12.048

Schiaroli, A., Mata, C., Scarponi, G.E., Cozzani, V., Ustolin, F., 2023. Digital image processing for the estimation of the thermal power entering a liquid hydrogen tank exposed to a fire. Inst. Chem. Eng. Symp. Ser. 2023-Novem.

Seeram, E., 2019. Digital Image Processing Concepts, in: Digital Radiography. Springer, Singapore, pp. 21–39.

Sharma, A., Singh, P.K., Kumar, Y., 2020. An integrated fire detection system using IoT and image processing technique for smart cities. Sustain. Cities Soc. 61, 102332. https://doi.org/https://doi.org/10.1016/j.scs.2020.102332